

Formation Conditions of Leucite-Bearing Lavas in the Bolsena Complex (Vulsini, Italy): Research Data on Melt Inclusions in Minerals

A.T. Isakova^{a,✉}, L.I. Panina^a, F. Stoppa^b

^a V.S. Sobolev Institute of Geology and Mineralogy, Siberian Branch of the Russian Academy of Sciences,
pr. Akademika Koptyuga 3, Novosibirsk, 630090, Russia

^b Dipartimento di Scienze DiSPUTer, Università degli Studi G. d'Annunzio, via dei Vestini 30, Chieti Scalo (CH), 66100, Italy

Received 29 June 2017; received in revised form 9 November 2017; accepted 15 June 2018

Abstract—A melt inclusion study was carried out in the leucite-bearing tephriphonolite and phonolite lavas of the Bolsena complex in order to obtain direct data on the chemical composition of initial melts, their evolution, and their crystallization temperatures. It has been found that the initial melt for the considered rocks was of tephrite–basanite composition. Its crystallization began with the formation of clinopyroxene phenocrysts at 1205–1100 °C, then leucite and plagioclase crystallization took place at about 1120 °C and 1080–1060 °C, respectively. The initial tephrite–basanite melt was slightly enriched in volatile components (H₂O, F, SO₃, and Cl). During the crystallization of clinopyroxene, leucite, and plagioclase, the composition of the initial magma changed toward an increase in the contents of SiO₂, Al₂O₃, and K₂O and a decrease in the contents of FeO, MgO, and CaO, i.e., evolved toward phonolite. A similar evolution trend is typical of alkaline basic systems. The tephrite–basanite melt was probably the product of the crystallization differentiation of the parental mantle magma similar in composition to the leucite-bearing tephrite–basanite of the Montefiascone complex.

Keywords: leucite, tephriphonolite, phonolite, melt inclusion, Roman magmatic province, Vulsini

INTRODUCTION

Classical leucite-bearing volcanics are found in the Roman magmatic province (Foley et al., 1987), which consists of four large volcanic fields: Vulsini, Vico, Sabatini, and Coli-Albani (Peccerillo, 2005). Volcanism in this area is predominantly of an explosive character with multiple Plinian eruptions and subsidence caldera. It should be noted that the geodynamic situation of the Roman magmatic province is still at the center of theoretical controversies and not entirely understood. Most researchers consider the magmatism of the Roman magmatic province to be connected with subduction processes (Serri et al., 1993; Boari et al., 2009; etc.). Others (Hawkesworth and Vollmer, 1979; Cundari, 1994; Lavecchia and Stoppa, 1996; Castorina et al., 2000; Bell et al., 2003) agree with the supposition that potassic magmatism in this province appears to be intraplate and caused by deep tectonic faults of the Rhenish–Libyan rift system (Borodin, 1974; Kostyuk, 2001), and some others (Lustrino et al., 2011; Lavecchia and Bell, 2012; Bell et al., 2013) relate it to plume activity. The great amount of information on geological position, petrologic composition and geochemistry of alkaline magmatism of the Roman magmatic province

has been accumulated (Washington, 1906; Holm et al., 1982; Conticelli et al., 1991; Nappi et al., 1995; Gasperini et al., 2002; Peccerillo, 2005; Lavecchia and Bell, 2012; etc.).

This study will be concerned with the volcanic field of Vulsini, which lies in the north of the Roman magmatic province, occupies an area of 2280 km² and is comprised of four volcanic complexes: Paleo-Bolsena, Bolsena, Montefiascone, and Latera. Eruptions occurred from more than 100 epicenters including four calderas and the caldera lake of Bolsena. The volcano was active for the period 0.6–0.15 Ma. All the volcanic complexes are made up of lava streams from high-potassium to low-potassium series (mill, basanite, latite, trachytic, tephriphonolite, and phonolite), scorias, Plinian sediments and ignimbrites. Most researchers consider the occurrence of different rocks in the same Vulsini volcanic field to be caused mainly by the processes of fractional crystallization. The processes of crust contamination and magma mingling are not excluded (Barton et al., 1982; Varekamp and Kalamarides, 1989).

We have done melt inclusion studies in leucite-containing lavas of tephriphonolite and phonolite composition of the Bolsena complex in order to obtain direct information on chemical composition of starting melts, which participated in Vulsini volcanic field formation, and also on their evolution in the process of crystallization, and crystallization temperature ranges. The comparative analysis has been also conducted with the analogous study results of melt in-

✉ Corresponding author.

E-mail address: atnikolaeva@igm.nsc.ru (A.T. Isakova)

clusions in minerals of other volcanic complexes of the Roman magmatic province (Barton et al., 1982; Kamenetsky et al., 1995; Lima et al., 2000).

Similar melt inclusion studies of leucite rocks from Vulcini were conducted only on olivine phenocrysts from volcanic scorias of potassic-basanite composition from the Montefiascone complex (Kamenetsky et al., 1995). The problems concerning initial magma composition remained unresolved. In particular, it concerns the content of rare and rare earth elements, the enrichment with volatile components, evolution and mantle sources. Numerous studies of melt inclusions in minerals of leucite-bearing volcanics mainly deal with the rocks from the Vesuvius (Cioni et al., 1998; Webster et al., 2001; etc.) and the Roccamonfina (Lima, 2000; etc.) volcanos.

MATERIALS AND METHODS

The content of the petrographic elements in the studied rocks was determined by X-ray fluorescence analysis (RFA) by research associate, Dr. N.G. Karmanova. To carry out the analysis, VRA-20R and ARL-9900-XP X-ray fluorescence spectrometers were used. The detection limits for the most analyzed samples reached 0.01 wt.%, and for Na₂O and MgO—0.04 wt.% and 0.05 wt.%, respectively.

To conduct integrated melt inclusion study, thin sections and platelets polished from both sides of tephriphonolite and phonolite from the Bolcena complex were prepared. The optical studies of thin sections and polished platelets were carried out in transmitting and backscattered light using an Olympus BX51 polarization microscope.

The mineral inclusions were heated in the heating stage with a silite heater at the ambient temperature up to 1400 °C under permanent microscopic observation. The microthermal chamber was calibrated with the use of melting temperatures of pure salts, such as K₂Cr₂O₇ (398 °C), NaCl (800 °C), Au (1065 °C), and Mn (1245 °C). The accuracy of the temperature definition amounted to ±10 °C. The time of heating the mineral inclusions was on average 40–60 min. The process of heating the inclusions in clinopyroxene was started with softening of the inclusions glass. Then the melting of daughter clinopyroxene from the vacuole walls was observed and, finally, the gas bubble shrank and disappeared at 1100–1200 °C. The estimates which remained stable at the experiments repetition were taken for homogenization temperature. While the inclusions were being quenched, shrinkage of the bubble appeared. The experiments of inclusions homogenization in leucite turned out to be less successful. In time of heating daughter phases were melting and the gas bubble started to shape. The inclusions homogenization was completed only once at 1100 °C. In other cases, to avoid the greatest probability of decrepitation the inclusions, they were heated until the disappearance of the last crystal phase followed by the decrease of the gas bubble at the temperature up to 1120–1150 °C.

Chemical analysis of rock-forming minerals, crystallites and glasses in heated/unheated silicate inclusion melts was carried out using a TESCANMIRA 3MLUc scanning electron microscope (SEM), and the INCAEnergy 450+ (Oxford Instrumental Analytical Ltd.) software and microprobe analysis technique applied on a Cameca Camebax Micro microprobe analyzer. Viewing conditions with the TESCANMIRA 3MLU SEM are the following: accelerating voltage 20 kV, the probe current 1 nA. Simple oxides, metals and minerals were used as a standard for the most elements: SiO₂ (Si, O), Al₂O₃ (Al), diopside (Mg, Ca), albite (Na), orthoclase (K), Ca₂P₂O₇ (P), BaF₂ (Ba, F), Cr₂O₃ (Cr), pyrites (S), Ti⁰, Fe⁰, Mn⁰, Zn⁰, and others. Co⁰ was used for quantitative optimization (normalization by probe current and spectrometer calibration by the supplied energy). The matrix time on minerals is 20 s, and for silicate glasses—60 s. Viewing conditions for “Camebax-micro” microprobe analyzer: current intensity of 30–40 nA, accelerating voltage 20 kV, electron beam diameter 2.5–3 μm. To calibrate the analyzer before the experiments, the viewing of standards took place, i.e. natural minerals with strictly determined concentrations of certain elements (diopside, albite, and orthoclase). The elements detection limits were estimated as (wt.%): SiO₂—0.009; TiO₂—0.036; Al₂O₃—0.012; FeO—0.019; MgO—0.013; MnO—0.022; CaO—0.010; Na₂O—0.020; K₂O—0.010; BaO—0.105; SrO—0.019; P₂O₅—0.008; Cl—0.011; SO₃—0.011. The error rate of X-ray spectral analysis on the microanalyzer did not usually exceed 2 wt.%, if homogeneous and rather large bodies were examined. The detection error could reach up to 4–5 wt.% for the compositional analyses of mineral inclusions. All analytical studies were carried out at the CUC of Multielement and Isotope Research of IGM SB RAS, Novosibirsk. The technique of secondary ion mass spectrometry (SIMS) was applied to determine the content of volatile components (H and F) in the glass inclusions of clinopyroxene, in size not less than 30 μm, with the use of ion microprobe in accord with A.B. Sobolev’ methodology (Sobolev, 1996). Detections were carried out at the Yaroslavl Branch of the Institute of Physics and technology RAS.

VOLCANO GEOLOGY AND PETROGRAPHIC ROCKS DESCRIPTION

In the result of field works, gravitational anomalies and well studies, four main volcanic complexes were distinguished (Nappi et al., 1991) in the Vulcini volcanic field: Paleo-Bolsena (0.6–0.45 Ma), Bolsena (about 0.49–0.32 Ma), Montefiascone (0.3–0.2 Ma), and Latera (0.38–0.15 Ma). Several pyroclastic products and lava flows (not referred to the above mentioned complexes) were detached to form a separate complex—the Southern Vulcini (Fig. 1).

According to (Nappi et al., 1991) the Vulcini volcanic field is characterized with a few volcanic cycles, as follows: (i) a starting phase with the eruption of effusive leucite-containing lava flows referred to the Strombolian-type of the

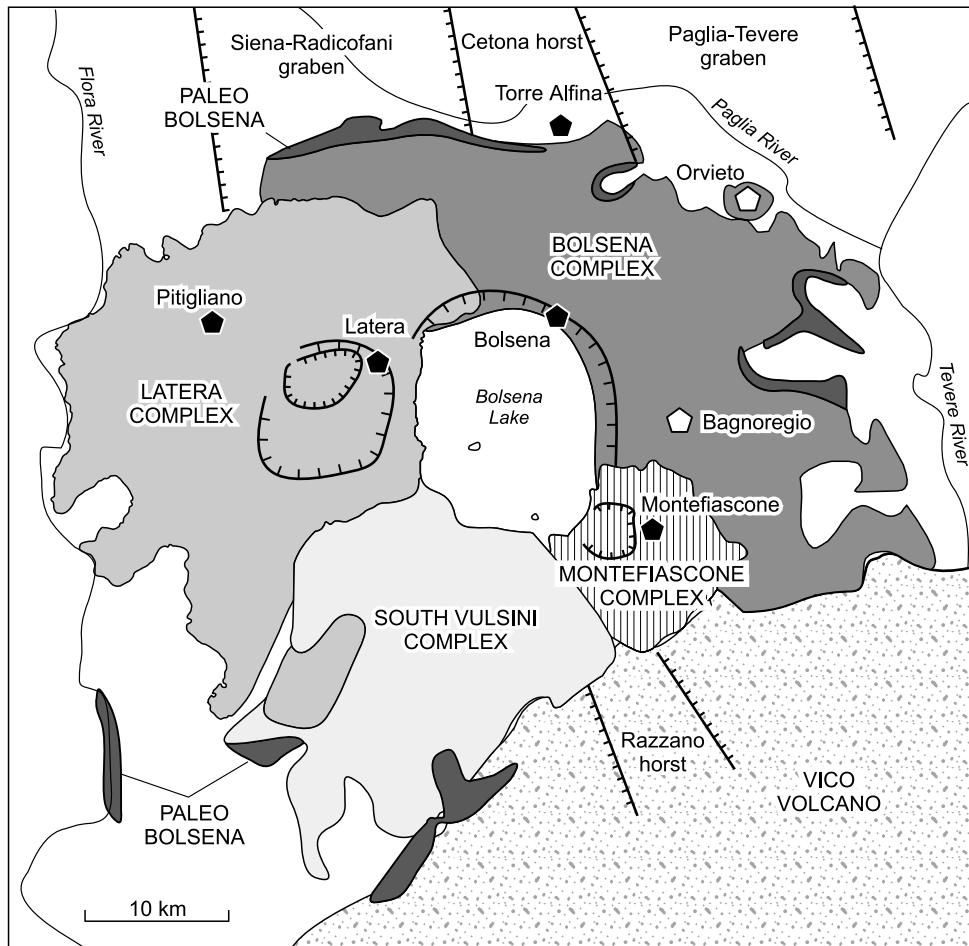


Fig. 1. The contour map of the Vulsini volcanic field (Peccerillo, 2005).

volcanic activity; (ii) explosive Plinian-type volcanic activity in the vicinity to the cross-section of large regional faults; (iii) the final stage distinguished by volcanic collapse caused by hydromagmatic and/or magmatic activity (Gupta, 2015).

The eastern and northeastern sectors of Vulsini are composed of the products from the Bolsena volcanic complex (Fig. 1). They are represented by flows of lava, Strombolian-type volcanic scorias, Plinian deposits, thick ignimbrite formations and hydrovolcanic products predominantly from high-potassium series including: leucite basanites, leucites, tephrites, phonolites, and trachyte and to a less extent—latites and shoshonites. The greatest part of all the products was erupted from the caldera of Bolsena Lake (Peccerillo, 2005), which appears to be the most ancient among all the calderas of Vulsini.

The subject of the current research are the Bolsena complex eruption products of the earliest age; these are the samples of lava flows of leucite-bearing tephriphonolite selected in the area of Orvieto. In accordance with the petrographical description, these rocks have a resemblance with the products from the Buon Vadgio lava flow with large leucite phenocrysts (up to 1 cm) described in (Varekamp, 1980) and with the age of 0.41 Ma (Everden and Curtiss, 1965). For

comparison, we have also studied the samples of leucite-bearing phonolites obtained from the same complex in the area of Bolsena Lake. Detailed petrographic studies of both rock types have revealed that they both have a porphyritic structure, contain the same mineral sets in different proportions. The texture of leucite-bearing tephriphonolite is more porous compared with that of phonolites with the large number of amygdules and cavities. Phenocrysts are abundant in leucite-bearing tephriphonolite and represented mainly by leucite, clinopyroxene, plagioclase and sometimes by alkaline feldspar. Leucite-bearing phonolites are comprised of sparse phenocrysts of leucite, plagioclase and clinopyroxene. The main bulk material in both rocks is made up of plagioclase laths, rounded crystals of leucite, hypidiomorphic crystals of clinopyroxene and xenomorphic grains of alkaline feldspar, and also by xenomorphic grains of titanomagnetite, and small crystals of apatites and crystalline glass.

Clinopyroxene, plagioclase and alkaline feldspar phenocrysts are zonal. Phenocrysts of clinopyroxene are short-columnar in shape and zonally colored: the cores are usually yellowish-green, green, but at the edges, the colors are getting darker and more saturated—dark green and brownish-

green. Phenocrysts with cores of a resorbed shape are of rare occurrence, they are light green colored, but their edges are dark green and brownish-green. The phenocrysts are small in size—up to 1–2 mm. Phenocrysts of leucite have idiomorphic tetragon trisoctahedron forms and their size can reach up to 5–8 mm. Phenocrysts of plagioclase are hypidiomorphic in form and often resorbed, with occasional fast-growing/dissolving textures and numerous inclusions simultaneously forming crystals with spongy cellular texture. They are small, up to 1 mm in size. Sparse phenocrysts of alkaline feldspar are larger (about 0.5 mm) and prismatic in shape. Chemical compositions of leucite-bearing tephriphonolite and phonolites are given in Table 1. The chemical compositions of leucite-bearing tephriphonolite (Table 1, an. 1) differs from that of leucite-bearing phonolites (Table 1, ans. 2–4) by higher concentrations of FeO, MgO, and CaO. It has much in common with leucite-bearing tephrite found in the Orvieto area (Table 1, ans. 5, 6) and differs only by low content of Na₂O (1.8 against 3.1–3.3 wt.%). Similar low concentrations of Na₂O are determined for tephrite leucite (Table 1, ans. 7, 8).

CHEMICAL COMPOSITION OF ROCK-FORMING MINERALS

Microprobe and scanning microscope studies have shown that the compositions of the observed minerals are nonhomogeneous.

Phenocrysts of **clinopyroxene** in tephriphonolite (Table 2, ans. 1–5; Fig. 2) are represented by diopsides, but in phonolite by diopsides-augite (Table 2, ans. 6–10). Diopsides compared with the latter contain more Al₂O₃, FeO, CaO and less SiO₂ and MgO. The grains of the ground mass

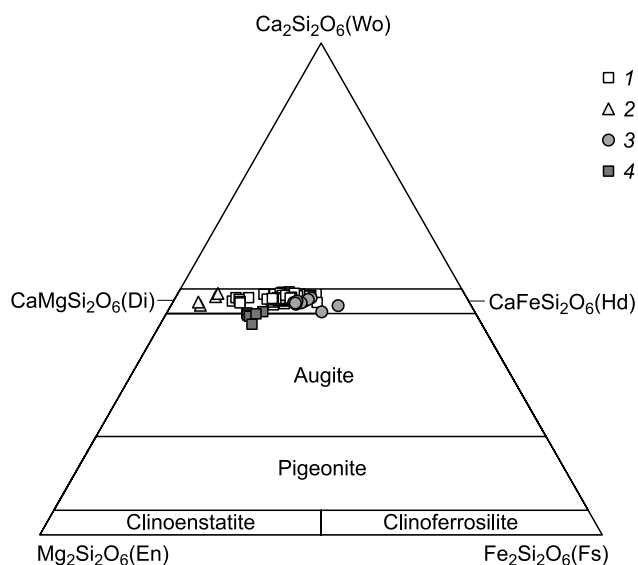


Fig. 2. Composition of Ca–Mg–Fe clinopyroxene (Morimoto, 1989). From tephriphonolite: 1, phenocrysts, 2, magnesian resorbed cores of phenocrysts, 3, grains of the groundmass; from phonolites: 4, phenocrysts.

are close in composition for both rocks and in comparison with phenocrysts usually contain more iron (Mg# up to 46), manganese (0.5–1.2 wt.% MnO) and sodium (0.6–1.4 wt.% Na₂O) (Table 2, ans. 13–17). It should be noted that the resorbed light green cores of phenocrysts in tephriphonolites (Table 2, ans. 11, 12) are characterized by high Mn-number (100Mg/(Fe + Mg)) up to 92 and contain up to 0.7 wt.% Cr₂O₃, 2.7–4.3 wt.% Al₂O₃, and 0.1–0.2 wt.% Na₂O.

Phenocrysts of **leucite** have a standard homogeneous composition in both rocks (Table 3, ans. 1–8). Phenocrysts of leucite in comparison with the grains of the ground mass (Table 3, ans. 9–11) contain more Na₂O (0.3–0.7 against 0.1–0.3 wt.%) and less FeO (0.3–0.4 against 0.5–0.7 wt.%).

The composition of **plagioclase** phenocrysts is close for both rocks and characterized by recurrent zonality (periodically repeating from direct to reverse) and alternating from bytownite to labradorite spar (An_{51–85}Ab_{14–46}Or_{1–4}) (Table 4, ans. 1–3, 18–20, Fig. 3). This type of zonality could be related to temperature fluctuations at the rise of water-saturated magma toward the surface, where not only decompression and magma crystallization occur, but also the mingling with hotter portions of magma (Streck, 2008). The rims of certain phenocrysts are represented by andesine (An_{45–49}Ab_{48–50}Or_{3–6}) (Table 4, ans. 4, 5). The composition of plagioclase laths mainly corresponds to (An_{23–28}Ab_{35–65}Or_{6–10}) (Table 4, ans. 6, 7, Fig. 3).

Large crystals of **alkaline feldspars** (Or_{47–62}Ab_{35–49}An_{3–7}) in tephriphonolites are characterized by specific zonality: big core zones (300–350 μm) are represented with homogeneous sanidine; intermediate zones are 20–30 μm thick and enriched with BaO (up to 4–5 wt.%), and rims/edge zones (20–30 μm) do not contain Ba (Table 4, ans. 8–10). Laths and grains of alkaline feldspars from groundmass are homo-

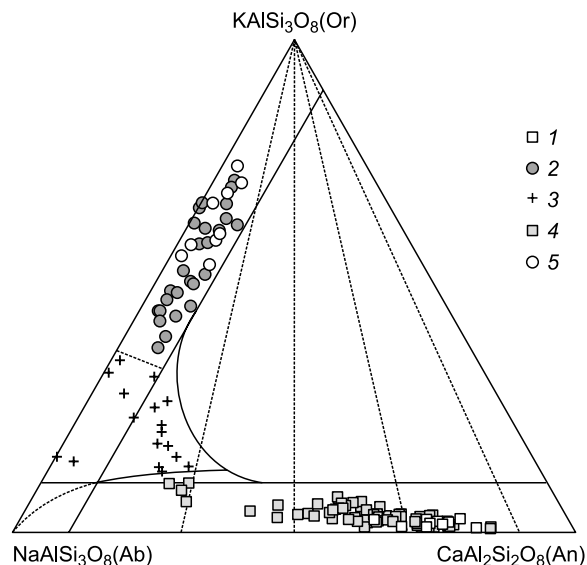


Fig. 3. Composition diagram of alkaline feldspar for solid solutions of albite–orthoclase–anorthite. From tephriphonolite: 1, plagioclase, 2, sanidine, 3, anorthoclase; from phonolite: 4, plagioclase, 5, sanidine.

Table 1. Chemical composition of the rocks from the Bolsena complex (Vulsini), wt.%

Component	1	2	3	4	5	6	7	8
	LTP	LP	LP	LP	LT	LT	TL	TL
SiO ₂	48.99	56.38	54.39	53.64	49.40	50.20	46.82	46.34
TiO ₂	0.94	0.64	0.58	0.51	1.00	0.90	0.74	0.76
Al ₂ O ₃	18.43	18.39	20.09	19.89	18.20	19.40	16.21	18.06
FeO _{tot}	8.25	4.36	3.71	3.82	8.05	7.29	7.32	7.48
MnO	0.16	0.10	–	0.15	–	–	0.15	0.17
MgO	4.36	1.30	0.97	0.83	3.30	2.80	5.35	3.38
CaO	8.32	4.11	3.67	3.59	7.90	7.20	11.19	9.66
Na ₂ O	1.76	3.14	3.96	2.89	3.10	3.30	1.85	2.40
K ₂ O	7.46	8.74	9.47	9.64	6.80	6.90	7.23	8.44
P ₂ O ₅	0.63	0.40	0.01	0.19	0.40	0.50	0.46	0.50
Total	99.30	98.04	96.85	95.15	98.15	98.49	97.32	97.19
Na ₂ O/K ₂ O	0.24	0.36	0.42	0.30	0.46	0.48	0.26	0.28
Mg#	0.35	0.23	0.21	0.18	0.29	0.28	0.42	0.31

Note. Rocks: LTP, leucite tephriphonolite; LT, leucite tephrite; TL, tephrite leucitite; LP, leucite phonolite. Dash, element was not detected. Analyses: 1, 2, our data 3, 5, 6, after (Varekamp, 1979); 4, 7, 8, after (Barton et al., 1982).

Table 2. Chemical composition of clinopyroxene from the Vulsini leucite-bearing tephriphonolites and phonolites

Component	1	2	3	4	5	6	7	8	9	10	11	12	13	14	15	16	17
	PH	GM	GM	GM	GM	GM											
SiO ₂ , wt.%	49.05	46.97	47.28	46.97	44.41	50.68	50.03	49.77	48.12	49.55	53.16	50.52	47.24	47.54	47.04	45.15	48.95
TiO ₂	0.88	1.28	1.26	1.15	1.50	0.78	0.70	0.79	0.92	1.07	0.38	0.93	1.25	1.59	1.62	2.21	1.49
Cr ₂ O ₃	b.d.l.	0.65	0.33	b.d.l.	b.d.l.	b.d.l.	b.d.l.	b.d.l.									
Al ₂ O ₃	4.68	6.37	5.43	6.01	7.93	3.39	3.81	4.25	4.81	3.45	2.22	4.97	5.69	4.71	5.12	6.92	3.14
FeO _{tot}	9.45	9.99	10.86	11.90	13.33	8.12	8.58	10.06	9.28	9.72	2.79	4.31	11.09	12.38	12.54	13.20	15.48
MnO	0.43	0.28	0.49	0.68	0.43	0.33	0.31	0.43	0.19	0.29	b.d.l.	b.d.l.	0.47	0.58	0.66	0.60	1.16
MgO	12.05	11.30	10.78	9.80	8.91	13.84	14.17	13.00	13.35	14.19	17.13	15.39	10.71	10.21	9.72	8.88	7.44
CaO	22.64	22.76	22.48	22.25	22.04	21.57	21.95	21.68	21.69	20.79	23.49	23.32	22.49	21.49	21.40	21.52	20.40
Na ₂ O	0.47	0.52	0.82	0.72	0.70	0.38	0.37	0.50	0.47	0.49	0.16	0.12	0.56	0.96	1.18	0.91	1.40
Total	99.66	99.48	99.39	99.48	99.26	99.09	99.92	100.48	98.83	99.55	99.97	99.90	99.50	99.46	99.28	99.39	99.47
Si, RFU	1.840	1.768	1.786	1.784	1.697	1.898	1.856	1.848	1.808	1.849	1.935	1.852	1.788	1.807	1.791	1.727	1.894
Ti	0.025	0.036	0.036	0.033	0.043	0.022	0.020	0.022	0.026	0.030	0.010	0.026	0.035	0.045	0.046	0.064	0.043
Cr	0.000	0.000	0.000	0.000	0.000	0.000	0.000	0.000	0.000	0.000	0.019	0.010	0.000	0.000	0.000	0.000	0.000
Al	0.207	0.283	0.242	0.269	0.357	0.150	0.167	0.186	0.213	0.152	0.095	0.215	0.254	0.211	0.230	0.312	0.143
Fe	0.297	0.315	0.343	0.378	0.426	0.254	0.266	0.312	0.292	0.303	0.085	0.132	0.351	0.393	0.399	0.422	0.501
Mn	0.014	0.009	0.016	0.022	0.014	0.010	0.010	0.014	0.006	0.009	0.000	0.000	0.015	0.019	0.021	0.020	0.038
Mg	0.674	0.634	0.607	0.555	0.508	0.772	0.783	0.719	0.748	0.789	0.929	0.841	0.604	0.578	0.552	0.506	0.429
Ca	0.910	0.918	0.910	0.906	0.903	0.866	0.872	0.863	0.873	0.831	0.916	0.916	0.912	0.875	0.873	0.882	0.846
Na	0.034	0.038	0.060	0.053	0.052	0.028	0.027	0.036	0.034	0.035	0.011	0.008	0.041	0.071	0.087	0.067	0.105
Fe ³⁺	0.097	0.147	0.173	0.150	0.213	0.037	0.110	0.110	0.153	0.120	0.007	0.028	0.141	0.155	0.181	0.174	0.087
Fe ²⁺	0.199	0.167	0.170	0.228	0.213	0.217	0.157	0.203	0.139	0.183	0.078	0.104	0.210	0.238	0.218	0.248	0.414
Al ^{IV}	0.160	0.232	0.214	0.216	0.303	0.102	0.144	0.152	0.192	0.151	0.065	0.148	0.212	0.193	0.209	0.273	0.106
Al ^{VI}	0.047	0.051	0.028	0.053	0.055	0.048	0.022	0.034	0.021	0.001	0.030	0.067	0.042	0.018	0.021	0.039	0.038
Mg#	69	67	64	59	54	75	75	70	72	72	92	86	63	60	58	55	46
Wo, %	50	52	52	51	53	45.7	47	47	48.5	45	47.4	49	51	49	50	51	46
En	37	36	34	31	30	40.8	42.5	39	41.5	43	48	45	34	32.5	31	29	23
Fs	11	10	11	14	14	12	9	12	8	10	4	5.5	13	14.5	14	16	25
Aeg	2	2	3	3	3	1.5	1.5	2	2	2	0.6	0.5	2	4	5	4	6

Note. PH, Phenocryst: 1–5, in tephriphonolite, 6–10, in phonolite, 11, 12, core of phenocryst with high Mg-number tephriphonolite; GM, grain from ground-mass (13–17). Stoichiometric coefficients (RFU) were calculated by the number of cations. Mg# = 100·Mg/(Mg + Fe_{tot}); b.d.l., below detection limit.

Table 3. Chemical composition of leucite from leucite-bearing tephriphonolites and phonolites from Vulsini

Component	1	2	3	4	5	6	7	8	9	10	11
	PH	PH	PH	PH	PH	PH	PH	PH	GM	GM	GM
SiO ₂ , wt. %	57.25	56.09	54.49	55.5	55.16	56.68	55.15	56.03	55.85	56.71	57.10
Al ₂ O ₃	22.79	22.1	22.23	23.34	23.18	22.25	23.07	23.40	22.95	22.40	22.36
FeO _{tot}	0.31	0.33	0.43	0.41	0.37	0.28	0.29	0.28	0.52	0.66	0.53
CaO	b.d.l.	b.d.l.	b.d.l.	b.d.l.	0.02	b.d.l.	0.01	b.d.l.	b.d.l.	b.d.l.	b.d.l.
Na ₂ O	0.41	0.27	0.67	0.48	0.46	0.35	0.67	0.34	0.30	0.16	0.18
K ₂ O	18.75	20.27	20.37	20.98	21.54	19.67	20.74	20.92	20.39	20.07	19.83
Total	99.51	99.1	98.19	100.71	100.73	99.23	99.93	100.97	100.00	100.00	100.00
Si, RFU	2.053	2.043	2.014	2.001	1.997	2.052	2.003	2.009	2.020	2.044	2.052
Al	0.961	0.947	0.967	0.990	0.987	0.948	0.986	0.987	0.976	0.950	0.945
Fe	0.009	0.010	0.013	0.012	0.011	0.008	0.009	0.008	0.016	0.020	0.016
Ca	0.000	0.000	0.000	0.000	0.001	0.000	0.000	0.000	0.000	0.000	0.000
Na	0.028	0.019	0.048	0.034	0.032	0.025	0.047	0.024	0.021	0.011	0.012
K	0.858	0.943	0.962	0.966	0.995	0.909	0.962	0.957	0.941	0.924	0.910

Note. PH, phenocryst deposits: 1–5, in tephriphonolite, 6–8, in phonolite; GM, grain from groundmass of tephriphonolites (9–11). Stoichiometric coefficients (RFU) were calculated by the number of oxides; b.d.l., below detection limit.

geneous in composition and corresponds to sanidine and anorthoclase (Or_{22–50}Ab_{46–63}An_{4–16}) (Table 4, ans. 11, 12; Fig. 3). Chadacryst found in phenocrysts of clinopyroxene (Table 4, ans. 13, 16), leucite (Table 4, ans. 14, 17) and plagioclase (Table 4, an. 15) from tephriphonolites are represented by sanidine with high content of BaO (1.2–6.5 wt.%) and rarely by anorthoclase and barium feldspar. Chadacryst composition of alkaline feldspar in phenocrysts of clinopyroxene (Table 4, ans. 21, 22) and plagioclase (Table 4, ans. 23, 24) from phonolites is consistent with sanidine and, in contrast to these ones in tephriphonolite, contains lower concentrations of BaO (up to 1 wt.%).

The **titanomagnetite** grains contain up to 8% of aluminum-spinel and up to 11% of ulvospinel components and small quantities of V₂O₃ (0.3–0.8 wt.%), MnO (1.2–4.7 wt.%), and MgO (up to 2 wt.%).

The impurity of rare earth elements (0.8–2.7 wt.% Ce₂O₃, to 1.2 wt.% La₂O₃, 0.3–1.0 wt.% Nd₂O₃, to 0.4 wt.% Pr₂O₃, 0.5 wt.% ThO₂), fluorine (4.1–5.4 wt.%), sulfur (0.5–1.4 wt.%), and chlorine (up to 0.1 wt.%) is detected in **apatite**.

MELT INCLUSIONS IN MINERALS

To obtain direct information on the composition of the initial melt, its evolution, the proceeding process and crystallization temperature, the primary melt inclusions (Fig. 4) were detected in phenocrysts of the studied rocks, such as clinopyroxene, leucite and plagioclase. The primary melt inclusions in **clinopyroxene** tend to position azonally in phenocrysts and prove to be glassy with a gas (shrinkage) bubble and rarely contain accessory minerals—apatite and magnetite. The sizes of inclusions vary from 10 × 10 to 40 × 60 μm (Fig. 4a, b). According to heating experiment results, the temperature of inclusion homogenization lies in the

range of 1100–1205 °C in tephriphonolites and 1160–1190 °C in phonolites.

The primary melt inclusions in phenocrysts of **leucite** tend to position along growth zones of host mineral and appear to be finely recrystallized (Fig. 4c). They are usually small in size ~10 × 12 μm, and they seldom reach 40 × 30 μm. Clinopyroxene were occasionally found as an accessory mineral in inclusions from leucite, its composition is close to that of phenocryst. It evidences about the simultaneously crystallization of clinopyroxene and leucite. Homogenization of inclusions in leucite has been accomplished only once at 1100 °C in tephriphonolites. In other cases, due to their frequent decrepitation, the inclusions are heated at elevated temperatures (up to 1120 °C) until the disappearance of the last daughter phase followed by the decrease of a gas bubble (Fig. 4d).

Partially recrystallized melt inclusions in phenocrysts of **plagioclase** were detected only in phonolites (Fig. 4e). They varied in size from 30 × 5 to 4 × 1 μm. They contain daughter sanidine, amphibole, residual glass and a gas phase. Homogenization of these inclusions occurs at 1060–1080 °C.

Glasses of heated melt inclusions in clinopyroxene from both rocks are close in composition, which varies from tephrites to trachytes-phonolites (Table 5, Fig. 5). However, the composition of glasses in tephriphonolites (Table 5, ans. 1–8) appears to be more basic in comparison with that one in phonolites (Table 5, ans. 9–16) and contains less SiO₂ (50.3–55.4 wt.% against 52.6–57.1) at closer values of MgO (2.0–4.5 wt.%) and Al₂O₃ (13.4–18.1 wt.%). Moreover, the glass of melt inclusions in clinopyroxene from tephriphonolites in comparison with that one from phonolites at equal concentration of SiO₂ contains more CaO (6.0–12.7 wt.% against 4.4–7.9 wt.%), MnO (0.2–0.4 wt.% against 0.1–0.2 wt.%), Na₂O (2.7–5.6 wt.% against 1.8–2.7 wt.%), TiO₂ (0.6–1.0 wt.% against 0.5–1.2 wt.%), Cl (0.08–0.16 wt.%

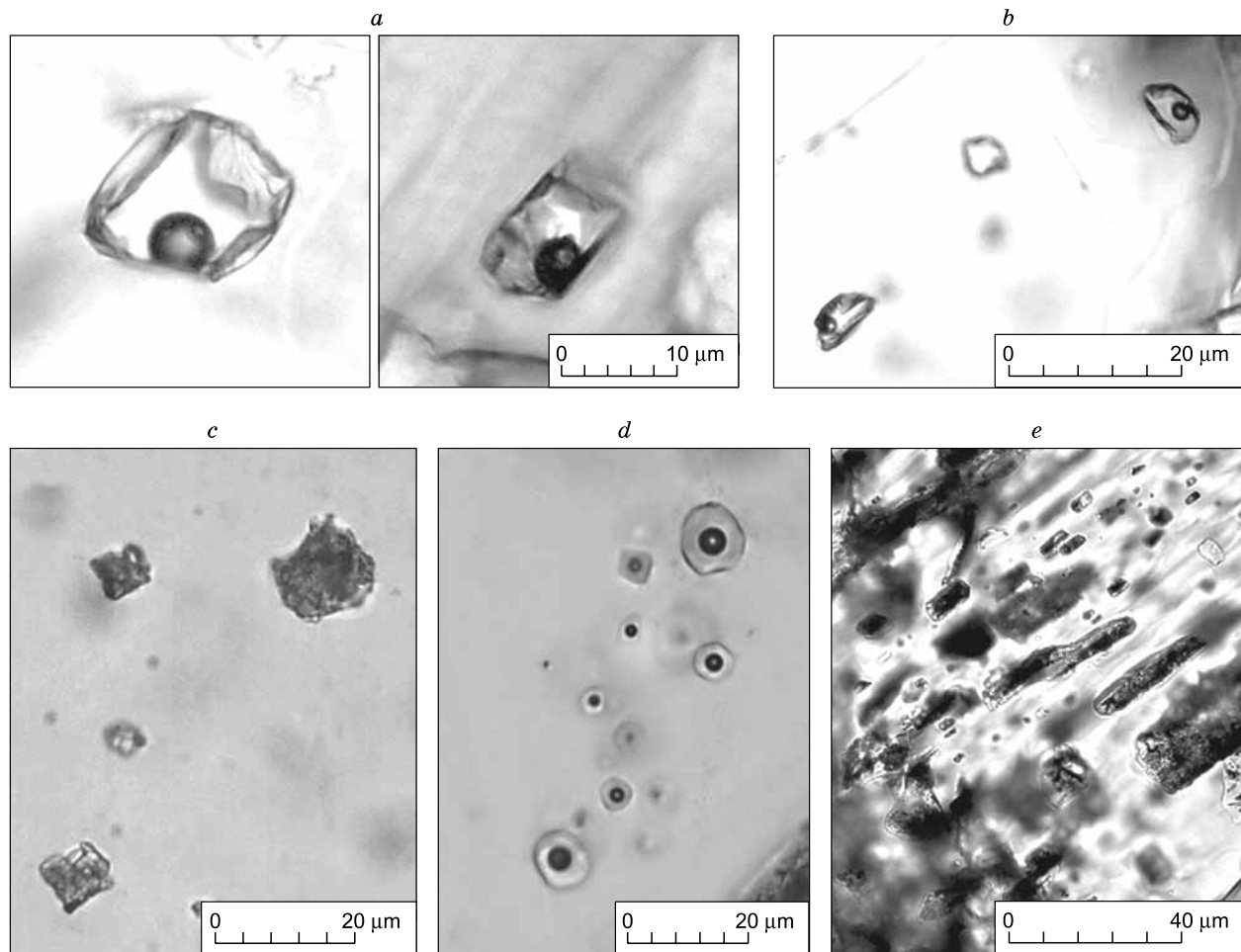


Fig. 4. Melt inclusions in phenocrysts of clinopyroxene (*a*, *b*), leucite (*c*, before heating, *d*, after heating) and plagioclase (*e*). SEM image in transmitting light.

against 0.4–0.06 wt.%) and less FeO (4.6–7.8 t.% against 4.5–8.2 wt.%), and K₂O (3.7–7.9 wt.% against 6.0–9.2 wt.%). The composition of glasses of heated inclusions from clinopyroxene of both rocks is also distinguished by P₂O₅ (up to 1.1 wt.%), SO₃ (up to 0.7 wt.%), F (up to 0.7–0.9 wt.%) and H₂O (0.5 wt.%). On condition that glass of heated inclusion is compared with unheated glass of inclusions in clinopyroxene (Table 6, ans. 1–17, Fig. 5), they contain much less Si, Al and alkalis and much more Fe, Mg, Ti, Mn, and Ca, that is they reflect the change in the melt composition in the result of the fractional crystallization of clinopyroxene on vacuole walls of inclusions.

When studying **glasses of melt inclusions in leucite** from tephriphonolites, 2 types of chemical compositions were determined: Mn-rich (Mg# 0.24–0.36; Table 7, ans. 1–9) and more Fe-rich (Mg# 0.06–0.13; Table 7, ans. 10–18). Inclusion with Mn-rich glasses (Table 7, ans. 1–9) are detected only in the central parts of the phenocrysts of leucite, and they sometimes contains accessory clinopyroxene, which does not melt during heating experiments. Inclusions with Fe-rich glasses (Table 7, ans. 10–18) are found in central, intermediate zone and rims of leucite. The composition

of Mn-rich glasses appeared to be close to the composition of clinopyroxene-hosted melt inclusions (Table 5). Moreover, from the center towards intermediate zone and rim in the composition of melt inclusions the contents of MgO and CaO tend to decrease, on the contrary, the contents of FeO, MnO, K₂O, and TiO₂ tends to increase. At closely spaced values of SiO₂ (53–55 wt.%), Al₂O₃ concentration is lower in Fe-rich glasses compared with the Mn-rich ones, but with the growth of SiO₂ content (>55 wt.%) its concentration rises concurrently (Fig. 6). It should be noted that the decrease of MgO concentrations from the center to the intermediate zones is rather dramatic: 2.8–4.2 and 0.5–1.8 wt.%, respectively (Table 7). It might be explained by the fact that the main part of clinopyroxene had already crystallized out at the crystallization stage of intermediate and edge zones of leucite phenocrysts that resulted in a sudden drop of MgO and CaO content in the melt. The glasses of heated inclusions trapped with leucite from phonolites (Table 7, ans. 19–26) have a composition that is either close to Fe-rich glasses or an intermediate one between Fe-rich and Mn-rich glasses of leucite inclusions from tephriphonolites (Fig. 6).

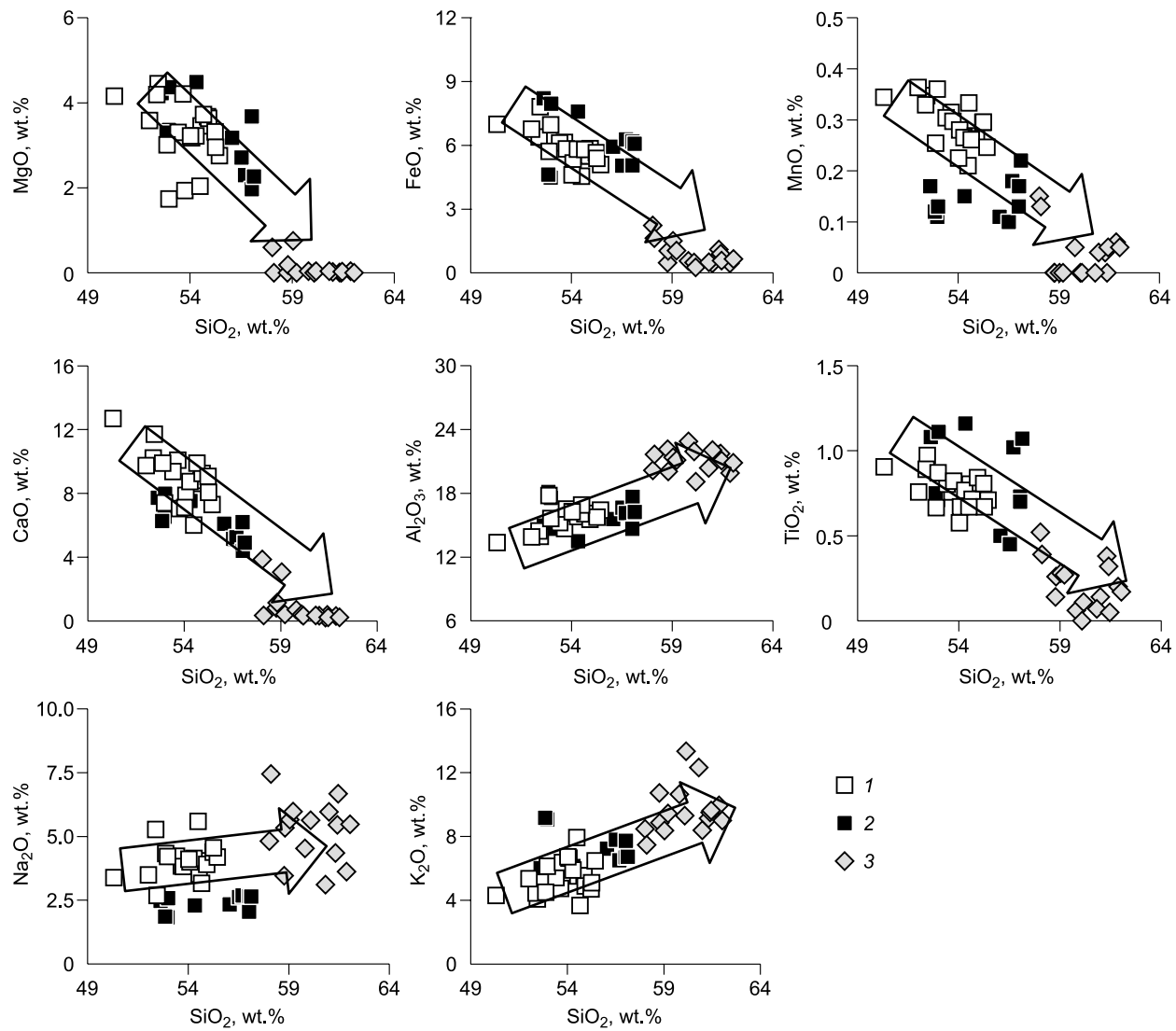


Fig. 5. Binary diagram of petrogenic oxides relations from SiO_2 in glasses of melt inclusions preserved in clinopyroxene phenocrysts. 1, heated inclusions from tephriphonolite; 2, heated inclusions from phonolite; 3, unheated inclusions from both types of the rocks. The alteration trend of glass composition is indicated with an arrow.

When compared with glasses of leucite from the same rock, **glasses of melt inclusions in plagioclase** (Table 8) from phonolites are characterized by low values of MgO, FeO, CaO, TiO_2 , MnO and high concentrations of Al_2O_3 and alkalis.

RESULTS AND DISCUSSION

The study has revealed that phenocrysts of clinopyroxene, plagioclase and alkaline feldspar in the examined rocks are zonal. Moreover, phenocrysts of plagioclase are marked by recurrent zonation and mostly being resorbed. They sometimes have a fast-growth/dissolution texture (crystals with spongy cellular texture). The cores of phenocrysts of clinopyroxene are prominently resorbed. These morphologi-

cal characteristics of phenocrysts and their compositions suggest the evolution of the initial melt, probable nonhomogeneity and feasible nonequilibrium crystallization at certain stages of its reformation.

According to the results of heating experiments, clinopyroxene in tephriphonolites crystallized at 1205–1100 °C, in phonolites at 1190–1160 °C; crystallization temperature for leucite is 1100 °C and for plagioclase—1080–1060 °C. Based on the chemical composition of minerals and contained melt inclusions, we tried to compare the obtained data with the estimates of P – T parameters of mineral crystallization calculated by the Putirka method (Putirka et al., 1996; Putirka, 2008). For the pair clinopyroxene–melt, P – T estimates were obtained by iteration method with the use of P1 and T1 formulae from the paper (Putirka et al., 1996), where temperature and pressure are interrelated. The calculation

Table 5. Chemical composition of glasses of heated melt inclusions in clinopyroxene from the Vulsini leucite-bearing tephriphonolite (1–8) and phonolite (9–16), wt.%

Component	1	2	3	4	5	6	7	8	9	10	11	12	13	14	15	16
SiO ₂	50.30	52.45	52.02	52.88	54.66	55.44	54.49	54.03	52.62	52.97	52.85	53.00	54.32	56.52	57.03	57.13
TiO ₂	0.90	0.97	0.76	0.67	0.71	0.71	0.67	0.58	1.08	0.71	0.75	1.11	1.16	0.45	0.70	1.07
Al ₂ O ₃	13.38	13.94	13.91	17.80	16.07	16.42	16.91	16.26	14.96	17.57	18.12	14.67	13.49	16.64	17.66	16.24
FeO _{tot}	6.99	7.81	6.76	5.71	5.81	5.10	4.55	4.61	8.21	4.48	4.62	7.96	7.59	5.05	5.06	6.07
MnO	0.34	0.35	0.36	0.25	0.26	0.25	0.21	0.22	0.17	0.11	0.12	0.13	0.15	0.10	0.17	0.22
MgO	4.16	4.45	3.59	3.01	3.72	2.76	2.04	3.22	4.23	3.36	3.30	4.37	4.49	2.71	1.97	2.27
CaO	12.70	11.72	9.75	9.90	9.91	7.31	6.02	7.12	7.73	6.54	6.27	7.98	7.52	5.15	4.40	4.92
Na ₂ O	3.38	2.69	3.49	4.32	3.17	4.19	5.59	4.10	2.47	1.83	1.86	2.58	2.29	2.62	2.66	2.64
K ₂ O	4.30	4.08	5.35	4.50	3.67	6.48	7.93	6.72	6.01	9.07	9.17	6.15	6.15	7.80	7.73	6.72
BaO	b.d.l.	0.27	0.30	b.d.l.	0.09	b.d.l.	b.d.l.	0.22	b.d.l.	0.21	0.14	0.10	0.12	0.19	0.24	b.d.l.
SrO	b.d.l.	0.04	0.13	0.14	0.04	0.03	b.d.l.	0.08	0.05							
P ₂ O ₅	1.10	0.14	b.d.l.	b.d.l.	b.d.l.	b.d.l.	b.d.l.	b.d.l.	0.05	0.80	0.82	0.20	0.17	0.07	0.32	0.31
SO ₃	0.25	0.22	0.10	b.d.l.	b.d.l.	b.d.l.	0.15	0.14	0.06	0.66	0.59	b.d.l.	0.06	0.12	0.17	0.12
Cl	0.12	0.13	0.15	0.16	0.08	0.16	0.14	0.15	0.04	0.06	0.05	0.06	0.06	0.05	0.05	0.05
F	b.d.l.	0.36	0.57	b.d.l.	b.d.l.	b.d.l.	0.35	0.10	–	–	–	–	–	–	–	–
Total	97.93	99.56	97.11	99.21	98.16	98.80	99.04	97.47	97.67	98.50	98.80	98.35	97.60	97.47	98.24	97.81
K ₂ O/Na ₂ O	1.27	1.52	1.53	1.04	1.16	1.54	1.42	1.64	2.43	4.96	4.93	2.38	2.69	2.98	2.91	2.55
Mg#	0.37	0.36	0.35	0.35	0.39	0.35	0.31	0.41	0.34	0.43	0.42	0.35	0.37	0.35	0.28	0.27
T _{hom} , °C	1190	1200	1190	1190	1190	1140	1165	1180	1190	1160	1190	1190	1160	1190	1160	1190

Note. Host clinopyroxene is represented by diopside in tephriphonolite, and by diopside-augite in phonolite. Dash, element was not detected; b.d.l., below detection limit.

Table 6. Chemical composition of glasses of unheated melt inclusions in clinopyroxenes from the Vulsini leucite-bearing tephriphonolites (1–10) and phonolites (11–17), wt.%

Component	1(2)	2	3(2)	4	5	6	7(2)	8	9(3)	10	11	12	13	14	15	16	17
SiO ₂	58.03	58.11	58.77	58.80	59.04	59.21	59.80	60.08	61.31	61.40	65.05	60.16	61.86	60.99	60.81	61.45	62.03
TiO ₂	0.52	0.39	0.14	0.26	0.28	0.27	0.06	b.d.l.	0.38	0.32	0.09	0.11	0.20	0.14	0.07	0.05	0.17
Al ₂ O ₃	20.17	21.66	22.13	20.05	21.38	21.13	22.87	21.95	21.64	21.74	17.81	19.10	19.91	22.07	20.38	21.07	20.87
FeO _{tot}	2.23	1.63	0.48	1.04	1.51	1.05	0.57	0.49	1.10	0.90	0.61	0.26	0.45	0.45	0.50	0.58	0.65
MnO	0.15	0.13	b.d.l.	b.d.l.	b.d.l.	b.d.l.	0.05	b.d.l.	0.04	b.d.l.	b.d.l.	b.d.l.	0.06	0.04	b.d.l.	0.05	0.05
MgO	0.60	b.d.l.	b.d.l.	0.19	0.75	b.d.l.	0.04	b.d.l.	0.01	b.d.l.	0.03	0.04	0.04	0.02	0.04	0.03	0.00
CaO	3.86	0.35	0.82	1.14	3.07	0.41	0.71	0.42	0.22	0.39	0.16	0.33	0.31	0.34	0.35	0.24	0.24
Na ₂ O	4.82	7.45	3.46	5.34	5.65	5.97	4.53	5.63	4.35	5.45	3.77	1.47	3.62	5.96	3.11	6.67	5.47
K ₂ O	8.48	7.48	10.73	8.86	8.38	9.44	10.65	9.31	9.13	9.51	10.33	13.35	9.95	8.39	12.32	9.63	9.01
BaO	0.31	b.d.l.	b.d.l.	0.18	b.d.l.	0.43	0.37	0.17	0.28	0.33	b.d.l.						
SrO	b.d.l.	0.24	b.d.l.	b.d.l.	b.d.l.	b.d.l.	b.d.l.										
P ₂ O ₅	0.08	b.d.l.	b.d.l.	b.d.l.	b.d.l.	b.d.l.	0.11	b.d.l.	0.06	b.d.l.	0.13	0.19	0.28	0.17	0.11	0.07	0.11
SO ₃	0.02	0.20	b.d.l.	b.d.l.	b.d.l.	0.17	0.12	0.20	0.12	0.15	0.06	0.07	0.06	0.09	0.03	0.07	0.08
Cl	0.17	0.22	b.d.l.	0.24	0.14	0.18	0.13	0.22	0.22	0.20	b.d.l.						
F	0.71	0.62	0.35	0.63	0.41	0.35	0.34	1.04	b.d.l.	0.27	–	–	–	–	–	–	–
Total	100.14	98.25	96.87	96.75	100.60	98.62	100.35	99.51	98.84	100.63	98.04	95.32	96.74	98.66	97.72	99.91	98.68
K ₂ O/Na ₂ O	1.76	1.00	3.10	1.66	1.48	1.58	2.35	1.65	2.10	1.74	2.74	9.08	2.75	1.41	3.96	1.44	1.65

Note. Dash, element was not detected. b.d.l., below detection limit. In brackets quantity of analyses done.

errors for pressure and temperature are equal to ± 1.4 kbar and ± 27 °C, respectively. For the pair plagioclase–melt, the temperature was calculated with the use of formulae (24a) and (26) from (Putirka, 2008) for the given pressure values

of 1–1.5 kbar (Varekamp, 1979; Barton et al., 1982; Pecerillo, 2005). The calculation errors for temperature lie in the range of ± 6 –10 °C. The calculated crystallization temperature values for tephriphonolites and phonolites are

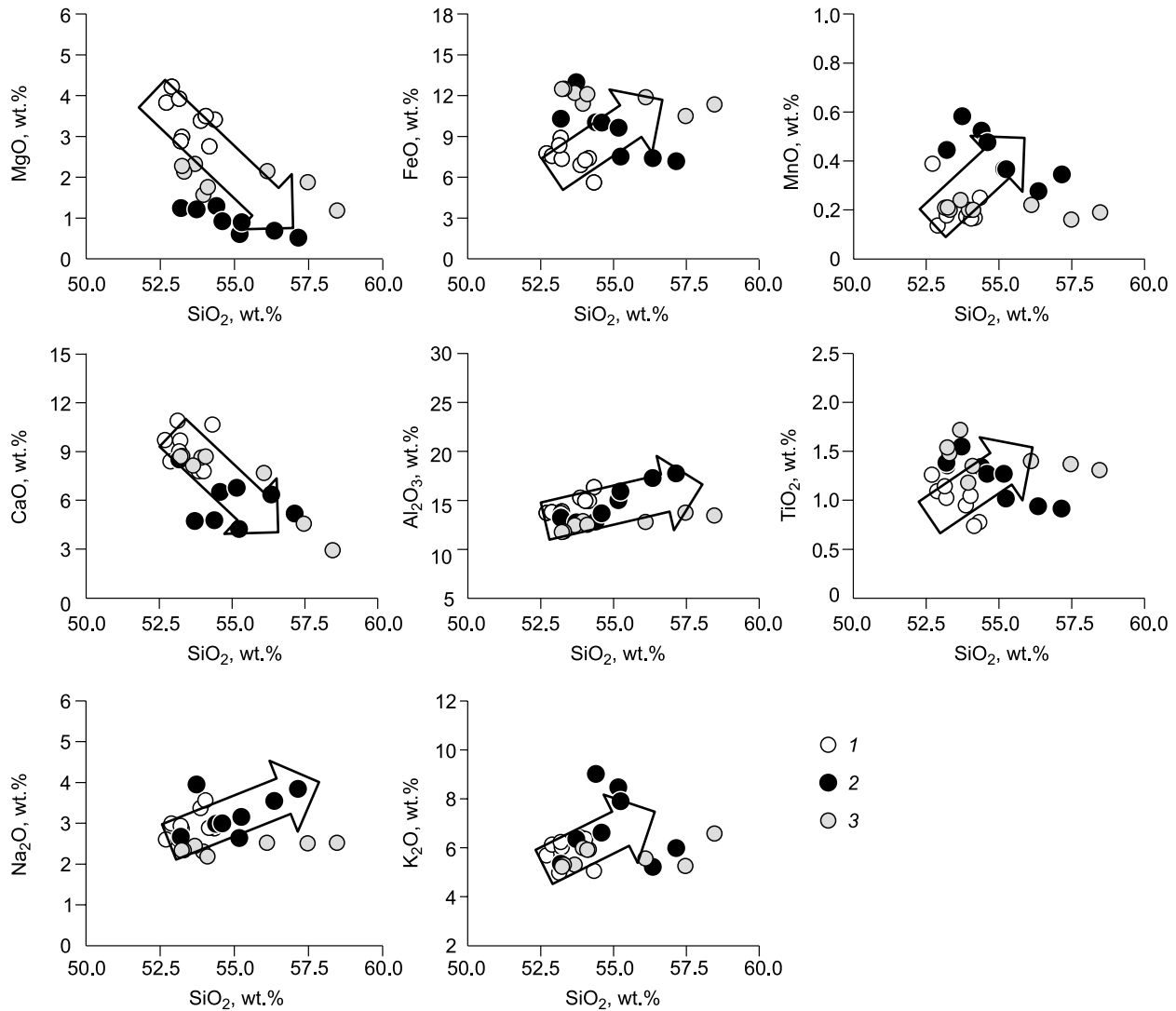


Fig. 6. Binary diagram of petrogenic oxides relations from SiO_2 in glasses of heated melt inclusions preserved in phenocrysts of leucite. From tephriphonolite: 1, Mn-rich, 2, Fe-rich; 3, from phonolite. The alteration trend of glass composition is indicated with an arrow.

closely spaced and equal: 1140–1223 and 1130–1225 °C, respectively. These values are quite comparable with our obtained temperatures of melt inclusions homogenization in clinopyroxenes from tephriphonolites and phonolites. The estimated pressure values by the barometer will be 6–12 kbar for tephriphonolites and 3–9 kbar for phonolites. With reference to our rocks, these pressure values are might be overestimated. According to (Varekamp, 1979; Barton et al., 1982; Peccerillo, 2005), pressure for Vulcini magma amounts to 1–1.5 kbar. For the pair plagioclase–melt from phonolites, and the given values of pressure of (1–1.5 kbar), the calculated temperature by formula (24) will be equal to 1070–1130 °C, and by formula (26)—1010–1070 °C. The obtained estimates are also comparable with temperatures of melt inclusions homogenization in plagioclase (1060–1080 °C). Consequently, the similar reproducibility of PT -calculated values and temperatures of melt inclusions homogenization in clinopyroxene and plagioclase points to the

fact that the obtained temperature interval (1060–1205 °C) indicates the real temperature of initial magma crystallization. These values are a little bit below the temperatures of olivine crystallization in more primitive tephrites of the Montefiascone complex (1192–1242 °C) (Kamenetsky et al., 1995) and comparable with clinopyroxene crystallization temperatures and that of clinopyroxene in leucite tephrites from the Roccamonfina volcano of the Roman magmatic province (1185–1250 °C) (Lima, 2000).

In accordance with the final data obtained on the chemical composition of heated melt inclusions glasses in minerals, we assume that the melts trapped by clinopyroxene are the most Mn-rich. In contrast, the melts preserved in plagioclase are the least Mn-rich, and the melts in leucite have an intermediate composition.

Based on the obtained data, the composition of the initial melt complies with tephrite-basanitic, and to the extent of clinopyroxene, leucite, and plagioclase crystallization it was

Table 7. Chemical composition of glasses of heated* melt inclusions in leucites from the Vulsini leucite-bearing tephriphonolites (1–18) and phonolites (19–26), wt.%

Component	1	2	3	4	5	6	7	8	9	10	11	12	13
SiO ₂	52.70	52.89	53.23	54.33	53.19	54.15	53.14	53.87	54.03	51.48	53.20	53.73	54.40
TiO ₂	1.26	1.09	1.35	0.78	1.03	0.74	1.14	0.95	1.04	1.82	1.38	1.55	1.34
Al ₂ O ₃	13.73	13.82	13.89	16.36	13.71	14.97	13.44	15.27	14.96	10.54	13.24	12.77	12.83
FeO _{tot}	7.76	7.57	7.37	5.62	8.90	7.41	8.35	6.91	7.27	11.92	10.29	13.00	10.05
MnO	0.39	0.14	0.46	0.25	0.18	0.17	0.21	0.17	0.16	0.66	0.44	0.58	0.52
MgO	3.83	4.22	2.99	3.41	2.88	2.76	3.92	3.39	3.50	1.75	1.24	1.21	1.29
CaO	9.70	8.40	9.68	10.66	9.01	8.68	10.88	7.80	7.80	7.19	8.51	4.74	4.78
Na ₂ O	2.61	2.99	2.87	2.87	2.94	2.89	2.60	3.38	3.56	3.28	2.67	3.95	2.98
K ₂ O	5.69	6.12	6.02	5.06	6.23	5.93	4.99	6.42	6.36	7.23	5.33	6.34	9.01
BaO	b.d.l.	b.d.l.	0.11	0.25	b.d.l.								
P ₂ O ₅	0.24	0.45	0.24	b.d.l.	0.37	0.30	0.44	0.46	0.43	0.28	b.d.l.	b.d.l.	0.11
SO ₃	b.d.l.	0.15	0.81	b.d.l.	0.15								
Total	97.91	97.68	98.21	99.59	98.45	97.98	99.09	98.62	99.09	96.31	97.12	97.93	97.45
K ₂ O/Na ₂ O	2.18	2.05	2.10	1.76	2.12	2.05	1.92	1.90	1.79	2.20	2.00	1.61	3.02
Mg#	0.33	0.36	0.29	0.38	0.24	0.27	0.32	0.33	0.33	0.13	0.11	0.09	0.11
Component	14	15	16	17	18	19	20	21	22	23	24	25	26
SiO ₂	54.60	55.17	55.25	57.16	56.35	53.95	53.67	53.30	53.23	54.10	56.10	57.47	58.46
TiO ₂	1.27	1.27	1.02	0.91	0.94	1.18	1.72	1.48	1.54	1.35	1.40	1.37	1.31
Al ₂ O ₃	13.67	15.01	15.91	17.75	17.29	12.90	12.48	11.84	11.79	12.52	12.82	13.76	13.47
FeO	10.01	9.64	7.53	7.18	7.41	11.42	12.22	12.51	12.50	12.12	11.89	10.50	11.37
MnO	0.48	0.37	0.37	0.34	0.28	0.20	0.24	0.20	0.21	0.20	0.22	0.16	0.19
MgO	0.92	0.60	0.90	0.52	0.69	1.57	2.33	2.14	2.28	1.76	2.15	1.88	1.19
CaO	6.52	6.77	4.25	5.20	6.37	8.63	8.15	8.73	8.69	8.70	7.69	4.58	2.96
Na ₂ O	2.99	2.64	3.15	3.84	3.54	2.31	2.45	2.34	2.34	2.19	2.52	2.51	2.52
K ₂ O	6.61	8.46	7.89	5.98	5.21	5.99	5.31	5.31	5.22	5.92	5.56	5.26	6.58
BaO	0.22	b.d.l.	0.08										
P ₂ O ₅	b.d.l.	0.14	b.d.l.	b.d.l.	b.d.l.	0.60	0.49	0.53	0.57	0.50	0.46	0.42	0.63
SO ₃	0.30	0.30	0.41	0.25	0.30	0.08	0.08	0.10	0.06	0.07	b.d.l.	0.08	0.11
Total	97.58	100.38	96.68	99.14	98.36	98.83	99.14	98.48	98.43	99.43	100.81	97.99	98.87
K ₂ O/Na ₂ O	2.18	2.05	2.10	1.76	2.12	2.05	1.92	1.90	1.79	2.20	2.00	1.61	3.02
Mg#	0.08	0.06	0.11	0.07	0.09	0.12	0.16	0.15	0.15	0.13	0.15	0.15	0.09

Note. 1–9, Mn-rich glasses assigned predominantly to the central parts of leucite phenocrysts from tephriphonolite; 10–18, Fe-rich glasses assigned predominantly to the intermediate zones and rims of leucite phenocrysts from tephriphonolite; b.d.l., below detection limit.

*Homogenization temperature of inclusions ≥ 1120 – 1100 °C.

enriched in Si, Al, K and depleted of Mg and Ca, and also was changing toward trachyte–phonolites in accord with the laws of crystallization differentiation. It should be noted that Fe and Ti content in the melt during leucite crystallization started to grow (5.6–13.0 wt.% FeO and 0.9–1.8 wt.% TiO₂), reversely, Fe and Ti quantities reduced in the time of plagioclase crystallization (3.2–4.7 wt.% FeO and 0.5–0.6 TiO₂). The last trend could be connected with titanomagnetite crystallization during plagioclase formation. The composition of the initial melt (Table 5) preserved in clinopyroxene phenocrysts is close to the composition of more primitive melts from the Montefiascone complex. The latter contains (wt.%): 46.5–50.0 SiO₂, 12.4–14.2 Al₂O₃, 6.0–7.5 FeO, 8.4–9.7 MgO, 12.4–14.41 CaO, 1.1–1.6 Na₂O, 2.8–5.3 K₂O, 0.2–0.4 P₂O₅, 0.12–0.26 S, 0.03–0.05 Cl, i.e., they correspond to

leucite tephrite-basanites in composition (Varekamp and Kalamarides, 1989; Kamenetsky et al., 1995). According to (Foley, 1992; Kamenetsky et al., 1995), such melts are products of a metasomatized mantle source of mainly clinopyroxene–phlogopite composition enriched with incompatible elements and volatile components. According to (Gupta and Yagi, 1980), ultramafic leucite-bearing magma of the same composition can be generated from partial melting of garnet peridotite enriched in phlogopite and richterite. The mantle origin of the potassium magma has been confirmed by geophysical data. For instance, the determined depth of the parental magma generation can reach 120–140 km for the Roman magmatic province; but the same parameter is estimated at 300 km and more for the Mediterranean volcanoes including the Vesuvius (Andreeva et al., 1984). Consequently,

Table 8. Chemical composition of glasses of heated* melt inclusions in plagioclase from the Vulsini leucite phonolites, wt.%

Component	1	2	3	4	5	6	7
SiO ₂	52.05	52.31	53.11	53.82	54.03	54.04	56.25
TiO ₂	0.56	0.57	0.57	0.53	0.46	0.59	0.57
Al ₂ O ₃	21.30	21.78	20.88	22.75	21.09	20.85	19.56
FeO _{tot}	4.65	3.69	4.70	3.64	3.70	3.22	4.29
MnO	0.12	0.07	0.13	0.08	0.08	0.08	0.11
MgO	1.43	1.19	1.40	1.17	1.05	1.10	1.00
CaO	7.01	6.58	5.25	4.89	5.39	6.13	4.69
Na ₂ O	3.23	3.18	2.89	2.80	2.76	2.73	2.40
K ₂ O	6.61	7.55	7.30	8.46	7.95	7.94	7.36
BaO	b.d.l.	0.18	0.15	0.09	0.09	b.d.l.	0.12
SrO	0.24	0.24	0.22	0.18	0.25	0.22	0.23
P ₂ O ₅	0.24	0.21	0.23	0.14	0.12	0.15	0.17
SO ₃	0.10	0.05	0.06	0.05	0.07	0.06	b.d.l.
Cl	0.06	0.05	0.03	0.05	0.06	0.05	0.06
Total	97.60	97.65	96.92	98.65	97.10	99.16	96.81
K ₂ O/Na ₂ O	2.05	2.37	2.53	3.02	2.88	2.91	3.07
Mg#	0.24	0.24	0.23	0.24	0.22	0.25	0.19

Note. Composition host plagioclase for analyzed inclusions is: An_{72–76}Ab_{22–25}Or_{1,9–2,7}; b.d.l., below detection limit.

*Homogenization temperature of inclusions in plagioclase ranges from 1060 to 1080 °C.

evolutional transformation (primarily crystallization differentiation) of the parental ultramafic ultrapotassic mantle magma seems to be the result of the melts appearance, from which leucite-bearing tephriphonolites–phonolites lavas of Vulsini were crystallized.

It was determined that the presence of volatile components is characteristic for the initial tephrite-basanite melts, as follows: up to 0.5 wt.% H₂O, 0.6–0.9 wt.% F, up to 0.3 wt.% SO₃, and up to 0.2 wt.% Cl. In broader terms, the melts contain more Cl and F, but less SO₃ in comparison with more primitive melts of leucite-tephrite composition being preserved in Montefiascone olivines and in clinopyroxene of Roccamonfina (0.03–0.05 wt.% Cl, 0.1–0.4 wt.% F, 0.3–1.1 wt.% SO₃) (Kamenetsky et al., 1995; Lima, 2000). Fluorine is the main volatile component of the ultrapotassic rocks and has a positive correlation effect on the potassium content (Aoki et al., 1981). Fluorine (F) is also known to possess a polymerizing effect in ultrapotassic melts depleted of H₂O; on the contrary, HF dominates instead of F in water-containing melts and fulfills a function of a depolymerizing agent (Foley et al., 1986). The content of volatile components in melts (i.e., H₂O, Cl, and S) and their solubility influence the character of the eruption (Webster et al., 2003). For instance, relatively low content of H₂O, Cl, and S in the initial trachybasalt melt, and low ratio of S/Cl were likely to be a reason of a passive-type eruption on Vulsini, presented by lava flows and scorias. According to (Webster et al., 2001), it is the high content of H₂O (1.5–3.5 wt.%), Cl (0.4–0.6 wt.%), and SO₃ (about 0.6 wt.%) in phonolite–phonotephrite melt and mainly the high ratio of S/Cl that had the greatest impact on the explosive character of the Vesuvius eruption that happened 3.55 thousand years ago.

CONCLUSIONS

Crystallization of leucite-bearing tephriphonolites started with the formation of clinopyroxene from the homogenous tephrite-basanite magma at 1100–1205 °C. Then, leucite (~1120 °C) and plagioclase (1060–1080 °C) started to crystallize from the melt. The initial melt was slightly enriched in volatile components (H₂O, F, SO₃, and Cl). To the extent of clinopyroxene, leucite and plagioclase crystallization, the composition of the initial magma was changing toward the increase of SiO₂, Al₂O₃, K₂O and decrease of FeO, MgO, and CaO; consequently, its composition evolved in the direction of trachyte-phonolites. This trend of evolution is the most typical of alkaline-basalt systems.

The initial tephrite-phonolite melt could be a product of crystallization differentiation of the parental mantle magma, which is similar in composition with leucite-tephrite-basanite of the Montefiascone complex.

The research was supported by the Russian Federation President grant for the support of young scientists (No. MK 5016.2016.5), the Russian Foundation for Basic Research (No. 17-05-00285), and the Russian Science Foundation (No. 14-17-00602P).

REFERENCES

- Andreeva, E.D., Kononova, V.A., Sveshnikova, E.V., Yashina, P.M., 1984. Igneous Rocks. Vol. 2: Alkaline Rocks [in Russian]. Nauka, Moscow.
- Aoki, K., Ishikawa, K., Kanisawa, S., 1981. Fluorine geochemistry of basaltic rocks from continental and oceanic regions and petrogenetic application. *Contrib. Mineral. Petrol.* 76 (1), 53–59.

- Barton, M., Varekamp, J.C., Van Bergen, M.J., 1982. Complex zoning of clinopyroxenes in the lavas of Vulsini, Latium, Italy: Evidence for magma mixing. *J. Volcanol. Geotherm. Res.* 14 (3–4), 361–388.
- Bell, K., Castorina, F., Rosatelli, G., Stoppa, F., 2003. Large-scale, mantle plume activity below Italy: Isotopic evidence and volcanic consequences, in: EGS–AGU–EUG Joint Assembly (Nice, France, 6–11 April 2003), Abstract 14,217.
- Bell, K., Lavecchia, G., Rosatelli, G., 2013. Cenozoic Italian magmatism—Isotope constraints for possible plume-related activity. *J. South Amer. Earth Sci.* 41, 22–40.
- Boari, E., Tommasini, S., Laurenzi, M.A., Conticelli, S., 2009. Transition from ultrapotassic kamafugitic to sub-alkaline magmas: Sr, Nd, and Pb isotope, trace element and ^{40}Ar – ^{39}Ar age data from the Middle Latin Valley volcanic field, Roman Magmatic Province, Central Italy. *J. Petrol.* 50 (7), 1327–1357.
- Borodin, L.S., 1974. The Main Principles and Formations of Alkaline Rocks [in Russian]. Nauka, Moscow.
- Castorina, F., Stoppa, F., Cundari, A., Barbieri, M., 2000. An enriched mantle source for Italy's melilitite-carbonatite association as inferred by its Nd–Sr isotope signature. *Mineral. Mag.* 64, 625–639.
- Cioni, R., Marianelli, P., Santacroce, R., 1998. Thermal and compositional evolution of the shallow magma chambers of Vesuvius: Evidence from pyroxene phenocrysts and melt inclusions. *J. Geophys. Res.* 103 (B8), 18,277–18,294.
- Conticelli, S., Francalanci, L., Santo, A.P., 1991. Petrology of the final stage Latera lavas: mineralogical, geochemical and Sr-isotopic data and their bearing on the genesis of some potassic magmas in Central Italy. *J. Volcanol. Geotherm. Res.* 46, 187–212.
- Cundari, A., 1994. Role of subduction in the genesis of potassic basaltic rocks: a discussion paper on the unfashionable side of the role. *Mineral. Petrograph. Acta* 37, 81–90.
- Everden, J.F., Curtiss, G.H., 1965. K–Ar dating of late Cenozoic rocks in Italy and Africa. *Curr. Anthropol.* 6, 343–385.
- Foley, S.F., 1992. Petrological characterization of the source component of potassic magmas: geochemical and experimental constraints. *Lithos.* 28, 187–204.
- Foley, S.F., Taylor, W.R., Green, D.H., 1986. The role of fluorine and oxygen fugacity in the genesis of the ultrapotassic rocks. *Contrib. Mineral. Petrol.* 94 (2), 183–192.
- Foley, S., Venturelli, G., Green, D.H., Toscani, L., 1987. The ultrapotassic rocks: characteristics, classification, and constraints for petrogenetic models. *Earth-Sci. Rev.* 24, 81–134.
- Gasperini, D., Blichert-Toft, J., Bosch, D., Del Moro, A., Macera, P., Albarede, F., 2002. Upwelling of deep mantle material through a plate window: evidence from the geochemistry of Italian basaltic volcanic. *J. Geophys. Res.* 107, 2367–2371.
- Gupta, A.K., 2015. Origin of Potassium-Rich Silica-Deficient Igneous Rocks. Springer. DOI: 10.1007/978-81-322-2083-1.
- Gupta, A.K., Yagi, K., 1980. Petrology and Genesis of Leucite-Bearing Rocks. Springer. DOI: 10.1007/978-3-642-67550-8.
- Hawkesworth, C.J., Vollmer, R., 1979. Crustal contamination versus enriched mantle: $^{143}\text{Nd}/^{144}\text{Nd}$ and $^{87}\text{Sr}/^{86}\text{Sr}$ evidence from the Italian volcanic. *Contrib. Mineral. Petrol.* 69, 151–165.
- Holm, P.M., Lou, S., Nielsen, A., 1982. The geochemistry and petrogenesis of the Vulsinian district, Roman Province, Central Italy. *Contrib. Mineral. Petrol.* 80, 367–378.
- Kamenetsky, V., Metrich, N., Cioni, R., 1995. Potassic primary melts of Vulsumi (Roman province): evidence from mineralogy and melt inclusions. *Contrib. Mineral. Petrol.* 120, 186–196.
- Kostyuk, V.P., 2001. Alkaline Magmatism of the Siberian Platform Marginal Structure [in Russian]. Izd. SO RAN, Novosibirsk.
- Lavecchia, G., Bell, K., 2012. Magmatotectonic zonation of Italy: a tool to understanding Mediterranean geodynamics, in: Stoppa, F. (Ed.), *Updates in Volcanology—A Comprehensive Approach to Volcanological Problems*. InTech, pp. 153–178.
- Lavecchia, G., Stoppa, F., 1996. The tectonic significance of Italian magmatism: an alternative view to the popular interpretation. *Terra Nova* 8, 435–446.
- Lima, A., 2000. Experimental study on silicate-melt inclusions in clinopyroxene phenocrysts from Roccamonfina lavas (Italy). *Mineral. Petrol.* 70, 199–220.
- Lustrino, M., Duggen, S., Rosenberg, C.L., 2011. The Central-Western Mediterranean: Anomalous igneous activity in an anomalous collisional tectonic setting. *Earth-Sci. Rev.* 104 (1–3), 1–40.
- Morimoto, N., 1989. Nomenclature of pyroxenes. Subcommittee on pyroxenes. Commission on new minerals and mineral names. *Can. Mineral.* 27, 143–156.
- Nappi, G., Renzulli, A., Santi, P., 1991. Evidence of incremental growth in the Vulsinian calderas Central Italy. *J. Volcanol. Geotherm. Res.* 47, 13–31.
- Nappi, G., Renzulli, A., Santi, P., Gillot, P.Y., 1995. Geological evolution and geochronology of the Vulsini Volcanic District Central Italy. *Bull. Soc. Geol. Italy* 114, 599–613.
- Peccerillo, A., 2005. Plio-Quaternary Volcanism in Italy: Petrology, Geochemistry, Geodynamics. Springer. DOI: 10.1007/3-540-29092-3.
- Putirka, K., 2008. Thermometers and barometers for volcanic systems. *Rev. Mineral. Geochem.* 69 (1), 61–120.
- Putirka, K., Johnson, M., Kinzler, R., Longhi, J., Walker, D., 1996. Thermobarometry of mafic igneous rocks based on clinopyroxene-liquid equilibria, 0–30 kbar. *Contrib. Mineral. Petrol.* 123, 92–108.
- Serri, G., Innocenti, F., Manetti, P., 1993. Geochemical and petrological evidence of the subduction of delaminated Adriatic continental lithosphere in the genesis of the Neogene Quaternary magmatism of central Italy. *Tectonophysics* 223 (1–2), 117–147.
- Sobolev, A.V., 1996. Melt inclusions in minerals as a source of the fundamental petrological information. *Petrologiya* 4 (3), 228–239.
- Streck, M.J., 2008. Mineral textures and zoning as evidence for open system processes. *Rev. Mineral. Geochem.* 69 (1), 595–622.
- Varekamp, J.C., 1979. Geology and petrology of the Vulsinian volcanic area (Latium, Italy), in: *Geologica Ultraiectina*, No 22. Geol. Inst. Rijksuniversiteit, Utrecht.
- Varekamp, J.C., 1980. The geology of the Vulsinian area, Lazio, Italy. *Bull. Volcanol.* 43 (3), 489–503.
- Varekamp, J.C., Kalamarides, R.I., 1989. Hybridization processes in leucite tephrites from Vulsini, Italy, and evolution of the Italian potassic suite. *J. Geophys. Res.* 94 (B4), 4603–4618.
- Washington, H.S., 1906. The Roman comagmatic region, in: *Carnegie Inst. Publ.*, Issue 57, pp. 1–99.
- Webster, J.D., Raia, F., De Vivo, B., Rolandi, G., 2001. The behavior of chlorine and sulfur during differentiation of the Mt. Somma-Vesuvius magmatic system. *Mineral. Petrol.* 73, 177–200.
- Webster, J.D., De Vivo, B., Tappen, C., 2003. Volatiles, magmatic degassing and eruptions of Mt. Somma-Vesuvius: constraints from silicate melt inclusions, solubility experiments and modeling, in: De Vivo, B., Bodnar, R.J. (Eds.), *Melt Inclusions in Volcanic Systems*. *Developments in Volcanology*, Vol. 5, pp. 207–226.